On the Performance of Nyquist-WDM Terabit Superchannels Based on PM-BPSK, PM-QPSK, PM-8QAM or PM-16QAM Subcarriers

Gabriella Bosco, *Member, IEEE*, Vittorio Curri, *Member, IEEE*, Andrea Carena, *Member, IEEE*, Pierluigi Poggiolini, *Member, IEEE*, and Fabrizio Forghieri, *Member, IEEE*

***Abstract*—We investigated through simulations the performance of Nyquist-WDM Terabit superchannels implemented using polarization-multiplexed phase shift-keying based on 2 (PM-BPSK) and 4 (PM-QPSK) signal points or polarization-multiplexed quadrature amplitude modulation based on 8 (PM-8QAM) and 16 (PM-16QAM) signal points. Terabit superchannels are obtained through the aggregation of multiple subcarriers using the Nyquist-WDM technique, based on a tight spectral shaping of each subcarrier which allows very narrow spacing. We first studied the optimum transmitter/receiver filtering in a back-to-back configuration. Then we investigated the maximum reach for different spectral efficiencies, after nonlinear propagation over uncompensated links with lumped amplification. Performance for systems based on both standard single-mode fiber (SSMF) and large effective area non-zero dispersion-shifted fiber (NZDSF) has been analyzed. Assuming SSMF with 25-dB span loss, we found that PM-BPSK can reach 6480 km at a net capacity of 4 Tb/s across the C band. Conversely, PM-16QAM can deliver 27 Tb/s, but over 270 km only. Note that a lower span length, the use of Raman amplification and/or pure silica-core fibers (PSCFs) can significantly increase the maximum reach, but without changing the hierarchy among the performance of modulation formats. We also show that the maximum reachable distance is approximately 2/3 of the one achievable in linear propagation at the optimum launch power, regardless of the modulation format, spacing and fiber type. As additional results, we also verified that the optimum launch power per subcarrier linearly depends on the span loss, varies with the fiber type, but it is independent of the modulation format, and that the relationship between the maximum reachable distance and the span loss is almost linear.**

***Index Terms*—Coherent detection, nonlinear propagation, Nyquist-WDM, PDM-BPSK, PDM-QPSK, PDM-8QAM, PM-BPSK, PM-QPSK, PM-8QAM, PM-16QAM, PDM-16QAM, superchannel.**

Manuscript received August 21, 2010; revised October 27, 2010; accepted October 28, 2010. Date of publication November 09, 2010; date of current version December 24, 2010. This work was supported in part by CISCO Systems within a SRA programand in part by the European Union within the BONE-project ("Building the Future Optical Network in Europe"), a Network of Excellence funded by the European Commission through the 7th ICT-Framework Programme. The simulator OptSim™ was supplied by RSoft Design Group Inc.

G. Bosco, V. Curri, A. Carena, and P. Poggiolini are with Dipartimento di Elettronica, Politecnico di Torino 10129, Italy (e-mail: optcom@polito.it).

F. Forghieri is with Cisco Photonics Italy srl, Monza 20052, Italy (e-mail: fforghie@cisco.com).

Color versions of one or more of the figures in this paper are available online at http://ieeexplore.ieee.org.

Digital Object Identifier 10.1109/JLT.2010.2091254

I. Introduction

CURRENT conventional optical communications systems can operate at a maximum bit-rate of 40 Gb/s and are based on incoherent detection and wavelength-division multiplexing (WDM) with 50 GHz channel spacing, thus achieving a spectral efficiency (SE) of 0.8 bit/s/Hz. The increasing demand for data transmission capacity is however requiring to better exploit installed optical links operating in the C-band, fostering the search for transmission techniques with higher spectral efficiencies. A promising solution, already implemented in a first generation of commercial products [1], is the use of multilevel modulation formats based on polarization multiplexing (PM) and coherent detection that permit to increase the SE up to several bit/s/Hz [2]. Thanks to their limited bandwidth occupation such modulation formats can operate at channel spacing close to the baud-rate and can be combined in "superchannels". A superchannel is a set of very tightly spaced channels, that are typically termed "optical subcarriers". The superchannel is meant to go through routing devices as a single entity and its overall bit-rate can be in the Terabit per second range. Therefore, it could constitute a technology for implementing a future "Terabit Ethernet" [3]–[11].

Examples of Terabit superchannels can already be found in the literature. In [3] and [4] the subcarriers were electrically OFDM (Orthogonal Frequency-Division Multiplexing) modulated and the Terabit superchannels reached 600 and 400 km, respectively. In [5], 24 carriers were modulated using conventional PM-QPSK at 12.5 Gbaud each. Baud-rate subcarrier spacing was possible thanks to optical Coherent OFDM (Co-OFDM). A remarkable transmission distance of 7 200 km was reached.

In [6]–[8], instead of Co-OFDM, the Nyquist WDM concept was exploited. According to this principle, the subcarriers are spectrally shaped so that they occupy a very small bandwidth, close or equal to the Nyquist limit for inter-symbol interference-free transmission, which coincides with the baud-rate. Such narrow subcarriers can then be multiplexed at the transmitter (Tx) with spacing close or equal to the Baud-rate, with limited inter-subcarrier crosstalk. A theoretical comparison of the concept of Nyquist-WDM versus Co-OFDM can be found in [11]. In [7] and [8], 9 000 and 10 000 km Nyquist-WDM transmission was demonstrated, respectively, with rather different overall system features. These experiments suggest that Terabit superchannel transmission with Nyquist-WDM may be practically possible with trans-oceanic performance.

In this work, we concentrate on the study of superchannels obtained using the Nyquist-WDM technique, which, being more flexible to changes in the subcarrier spacing, is suitable to a study aimed at identifying a trade-off between capacity and reach. Since today's technology allows sampling up to about 60 GSamples/second [12], in this paper we assume to operate at a baud-rate (R_S) equal 27.75 Gbaud for all formats. We also assume an analog-to-digital converter (ADC) working at 2 samples per symbol (SpS), i.e., 55.5 GSamples/s. Such baud-rate corresponds to a net throughput of 25 Gbaud: the 11% overhead comprises a 4% due to the Ethernet protocol and a 7% for forward error correction (FEC) [13].

This work extends the results previously published in [14], where only three modulation formats and a single fiber type were analyzed. We compare here the performance of Terabit superchannels based on four modulation formats, all exploiting polarization-multiplexing (PM): binary phase shift-keying (PM-BPSK) [15], quaternary phase shift-keying (PM-QPSK) [16], quadrature amplitude modulation with 8 (PM-8QAM [17]) and 16 (PM-16QAM [18]) constellation points, having bit-rates (R_b) equal to 55.5 Gb/s, 111 Gb/s, 166.5 Gb/s and 222 Gb/s, respectively. For each format, we analyzed through simulation nonlinear propagation over a multi-span link based on standard single-mode fiber (SSMF) and large effective-area non-zero dispersion-shifted fiber (NZDSF) with lumped erbium-doped fiber amplifiers (EDFAs). The purpose was to assess the maximum transmission distance $L_{\max}$ ensuring a bit error-rate (BER) below the FEC threshold of $4 \cdot 10^{-3}$ [13], as a function of spectral efficiency and total capacity. With this aim, for each format we derive $L_{\max}$ for different values of subcarrier spacing (Δf), starting from the standard 50 GHz grid down to 27.75 GHz, i.e., down to a subcarrier spacing equal to the baud-rate R_S.

The paper is structured as follows. In Section II, we introduce the concept of Terabit superchannel and its applications in future optical communication systems. Then, in Section III, we describe the system setup used to obtain the simulative results presented in the subsequent sections. Section IV shows the results of the back-to-back optimization of the bandwidths of the Tx optical filter and the receiver (Rx) electric filter, as a function of the subcarrier spacing. The long-haul transmission results are shown and commented in Section V, where, for each modulation format and fiber type, a spectral efficiency versus maximum reach curve is derived. Several plots are also shown which highlight the dependence of performance on various relevant parameters of the transmission system, such as the average launch power per subcarrier, the maximum reach and the span loss, and give further insight into the impact of nonlinearities on system performance. Finally, in Section VI, we comment on our results and draw conclusions.

II. The Concept of Terabit Superchannels

Research has recently started to consider data aggregation by targeting 1 Tb/s per channel transmission. Even assuming the future availability of 100 GSamples/s ADCs (today's state-of-the-art is 60 GSamples/s), sending 1 Tb/s over a single carrier would require the use of PM-1024QAM. Such format would pose daunting problems, such as very poor sensitivity, extreme phase noise requirements, intolerance to non-linearity, hardware bandwidth problems, need for ultra-fast digital-to-analog converters (DACs) at the Tx and, ultimately, very short reach: less than few tens of km, even considering soft decoding FEC codes.

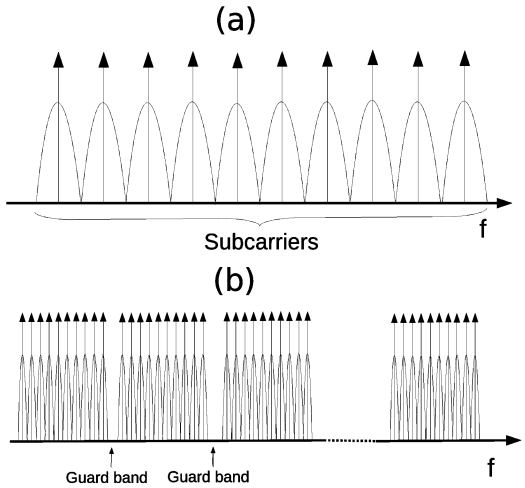

Fig. 1. Pictorial description of 1 Tb/s superchannel made up of 10 subcarriers (a) and comb of superchannels separated by a guard band in order to allow routing through OADMs and WSSs as a single entity. Depending on modulation format, the "delta" appearing at each subcarrier center frequency may or may not be present. In figure, the delta is shown just as a visual aid. (a) 1 Tbps Superchannel, (b) Aggregated Superchannels.

Terabit per channel transmission must then be tackled differently. A very recently emerged strategy is that of assembling a 1 Tb/s per channel by compounding a suitable number of "subcarriers" [3]–[11]. The Terabit channel so formed is actually called a *superchannel* and it is assumed to be routed through optical add-drop multiplexers (OADMs) and wavelength selective switches (WSSs) as a single entity. As an example, a 1 Tb/s superchannel can be obtained using 10 subcarriers, each carrying 100 G PM-QPSK. Subcarriers must be very densely packed in frequency to attain the highest possible spectral efficiency, which is one of the main challenges of superchannel transmission.

A pictorial description of the superchannel concept is displayed in Fig. 1. As stated in Section I, subcarrier aggregation can be obtained using either the Co-OFDM technique or the Nyquist-WDM technique. Co-OFDM uses an efficient subcarrier spacing exactly equal to the baud-rate, but it needs a large Tx/Rx electric bandwidth that is difficult to obtain with the state-of-the-art electronic equipment [10], [11]. Hence, such a technique is presently more suitable to lower baud-rate transmission [9]. With a baud-rate as high as 27.75 Gbaud, it seems more convenient to employ the Nyquist-WDM technique [11], that is based on reducing intra-subcarrier crosstalk by spectrally shaping the subcarrier at the Tx side and allowing a tradeoff between capacity and performance by extending or reducing the subcarrier spacing.

For practical reasons, the number of subcarriers in a superchannel should be kept reasonably low. Though integration is expected to greatly help, each subcarrier clearly needs a separate modulator, albeit perhaps integrated on a single chip with others. At the Rx, some devices could handle all subcarriers together, such as the 90-degree hybrid, and some integration can in fact

take place [19], but nonetheless essentially separate receivers for each subcarrier, at least at the digital signal processing (DSP) level, would be needed anyway.

Due to these practical constraints, a reasonable number of subcarriers is equal or less than ten. According to this guideline, a 1 Tb/s superchannel including FEC overhead could be made up of 10 subcarriers using PM-QPSK, operating at 27.75 Gbaud, carrying 111 Gb/s each. Also very interesting, though more challenging, is the possibility of achieving the same capacity by using fewer subcarriers, still operating at 27.75 Gbaud but resorting to a higher-order modulation format. For instance, only 5 subcarriers using PM-16QAM, delivering 222 Gb/s each, are needed to achieve the same raw capacity. Intermediate solutions using 7 subcarriers are possible with PM-8QAM. A preliminary simulative investigation of these three alternatives has been presented in [14] while a successful experiment of transmission of 10 subcarriers using PM-QPSK is described in [6]. In this paper, we include also the analysis on PM-BPSK as a performance reference for the other formats, even though it may not be a practicable option for generating 1 Tb/s superchannels, due to the high number of subcarriers (20) required to reach such capacity. Nevertheless, thanks to its good performance PM-BPSK may be an interesting option for a 400-Gb/s solution.

Nyquist-WDM superchannel complexity and overall bit-rate are clearly key aspects, but a third very important one is bandwidth efficiency. For the superchannel concept to make sense, subcarriers need to be very closely spaced. Having compact-bandwidth superchannels, and therefore high overall average spectral efficiency, is an essential target, that will be addressed in the following sections.

Note that the concept of Nyquist-WDM would require the use of very specific optical spectral shaping, i.e., of very specific optical filters, as discussed in [11]. Alternatively, ideal Nyquist-WDM can also be obtained by electrically shaping the modulator driving signals through a Tx DSP with digital-to-analog converters (DACs). In this paper, we chose to refrain from extremes and rather concentrate on technologies that are commercially available today. As a result, the Tx optical shaping filters are assumed to be fourth-order supergaussian filters. This clearly leads to somewhat suboptimum performance but conservatively shows what could be realistically done at present.

III. System Setup

The system scenario we analyzed is shown in Fig. 2(a). For all modulation formats, we used standard I-Q transmitters based on nested Mach–Zehnder modulators driven by non-return-to-zero (NRZ) signals. Each modulated subcarrier is spectrally shaped by a 4th-order Super-Gaussian optical filter, whose -3 dB bandwidth $B_{\rm opt}$ was optimized (see Section IV). The optical link is periodical and composed of $N_{\rm span}$ spans. Each span is composed of 90 km of transmission fiber followed by a variable optical attenuator (VOA) and by an erbium-doped fiber amplifier (EDFA) with noise-figure $F = 5$ dB that completely recovers the span loss $A_{\rm span}$. As transmission fibers, we considered both standard single-mode fiber (SSMF) and large effective area non-zero-dispersion fiber (NZDSF). The SSMF parameters are: loss coefficient $\alpha = 0.22$ dB/km, dispersion coefficient $D = 16.7$ ps/nm/km and nonlinear coefficient $\gamma = 1.3$ 1/W/km. For the NZDSF, we used: $\alpha = 0.22$ dB/km, $D = 3.8$ ps/nm/km and $\gamma = 1.5$ 1/W/km. We assumed no in-line dispersion compensation, because this has been shown to be the best configuration for polarization-multiplexed coherent modulation formats [20]–[22]. The total loss of each span $A_{\rm span}$ is due to two contributions. One is the loss of the fiber, 19.8 dB for both SSMF and NZDSF, and the other is the loss of the VOA.

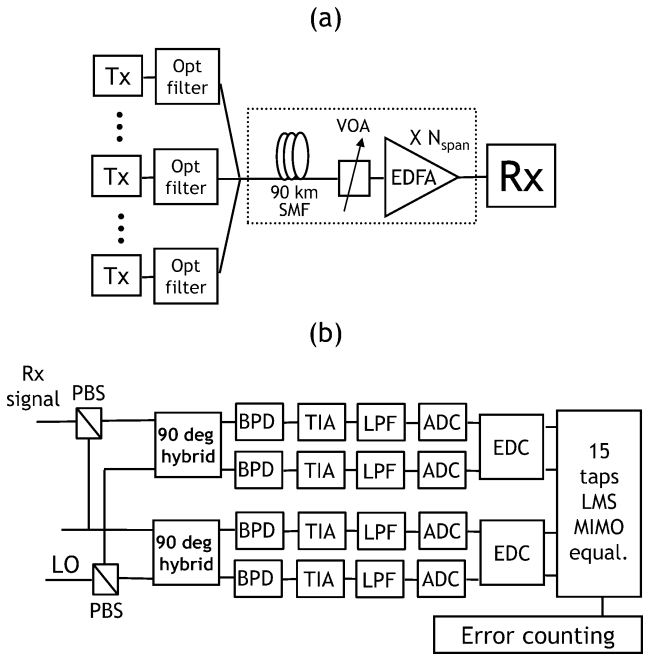

Fig. 2. Layout of the analyzed optical link (a) and of the coherent DSP based Rx used for the demodulation of a single subcarrier (b). SMF: single-mode fibre, VOA: variable optical attenuator, EDFA: erbium-doped fiber amplifer, LO: local oscillator, PBS: polarization beam splitter, BPD: balanced photo-detector, TIA: trans.impedance amplifier, LPF: low-pass filter, ADC: analog to digital converter, EDC: electronic dispersion compensator, LMS: least-mean square, MIMO: multiple-input multiple-output.

The Rx structure for each subcarrier is described in Fig. 2(b) and it is the same for the four considered modulation formats. It includes a local oscillator (LO), that is mixed with the incoming signal in two 90-degree hybrids [23], one for each polarization, in order to implement a polarization diversity Rx. No optical filtering is present at the Rx: the subcarrier is selected by changing the frequency of the LO. The alignment of the LO to the subcarrier center frequency is assumed ideal. Four balanced photo-detectors (BPD) are used to detect the received signal components. The signals are then filtered by a 5th-order low-pass Bessel filter (LPF), with optimized -3 dB bandwidth $B_{\rm Rx}$ (see Section IV). The power level of the signal at the input of the Rx guarantees the operation in the regime limited by amplified spontaneous emission (ASE) noise [24].

After detection and low-pass filtering each signal is sampled by an analog-to-digital converter (ADC), which is assumed to operate at 2 SpS. We also assumed infinite ADC resolution, so that there is no quantization penalty. After sampling, dispersion is fully and ideally compensated by the DSP. Then, the four signal components are processed by a MIMO (multiple-input multiple-output) equalizer [25], which consists of four complex 15-tap FIR filters. Besides state-of-polarization

(SOP) alignment, the butterfly equalizer is meant to recover other phenomena characterized by temporal "memory", such as residual chromatic dispersion and polarization mode dispersion. The equalizer FIR filter coefficients are estimated using the least mean square (LMS) algorithm, first using a training sequence, then operating on the base of the decided bit string in decision-directed mode. For each modulation format, a different LMS error function is applied taking into account its own signal constellation and bit mapping. The signals out of the equalizer can be used for decision and BERs were evaluated using direct error counting.

Simulations were carried out transmitting a full pseudo-random bit sequence (PRBS) of degree 16, for each data stream at 27.75 Gbaud on each subcarrier, corresponding to a total of 131072 simulated bits for PM-BPSK, 262144 bits for PM-QPSK, 393216 bits for PM-8QAM and 524288 bits for PM-16QAM. Different and uncorrelated PRBSs were used for each data stream of each subcarrier. PRBSs were also different from one subcarrier to another.

We simulated the propagation of 10 subcarriers employing 20 SpS: BER performance was probed on the center-left subcarrier (the 5-th). Fiber propagation was simulated using a full-band time-domain split-step method to solve dual-polarization Schrödinger equations.

IV. Back-to-Back Tx/Rx Optimization

The first step of the analysis was the study of back-to-back performance in an ASE noise limited scenario, in order to assess the impact of the subcarrier frequency spacing Δf on each modulation format. The performance was evaluated in terms of optical signal-to-noise ratio (OSNR), defined over a 0.1 nm noise bandwidth, required to achieve the target $\mathrm{BER} = 4 \cdot 10^{-3}$.

For each modulation format we considered a subcarrier spacing varying from the standard WDM spacing $\Delta f = 50$ GHz down to the baud-rate, i.e., $\Delta f = R_S = 27.75$ GHz. For every considered setup we performed a joint Tx/Rx optimization by varying the -3 dB bilateral bandwidth B_{opt} of the spectral shaping Tx optical filter and the -3 dB bandwidth B_{Rx} of the Rx low-pass electric filter, which has the double purpose of filtering noise and limiting the aliasing induced by the ADC sampling. For every pair $(B_{\mathrm{opt}}, B_{\mathrm{Rx}})$ we searched for the OSNR value corresponding to $\mathrm{BER} = 4 \cdot 10^{-3}$. An example of the results, obtained for PM-QPSK with $\Delta f = 33.3$ GHz, is shown in Fig. 3, where the contour plot of the required OSNR (in dB) is shown as a function of the normalized bandwidths $B_{\mathrm{opt}}/\Delta f$ and B_{Rx}/R_S. Similar results have been obtained for all Δf and for all analyzed modulation formats. The performance optimum always fell at approximately $B_{\mathrm{opt}} = \Delta f$ and $B_{\mathrm{Rx}} = 1/2\ R_S$. Such optimum values of filter bandwidths were used in both the subsequent back-to-back analysis and in all non-linear propagation investigations.

An explanation for such general behavior of the optimum bandwidth of the Tx optical filter is that a value of $B_{\mathrm{opt}} = \Delta f$ generates a shape of the transmitted signal spectrum corresponding to an optimum tradeoff between inter-subcarrier crosstalk and intra-subcarrier inter-symbol interference (ISI). Regarding the Rx electric filter, the value $B_{\mathrm{Rx}} = 1/2\ R_S$ is the closest to the optimum information theory "matched filter"

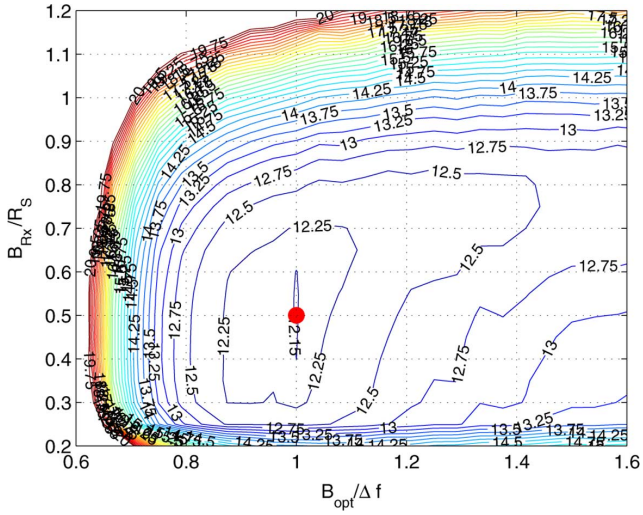

Fig. 3. Contour plot of the minimum OSNR (in dB) granting $\mathrm{BER} \leq 4 \cdot 10^{-3}$ in the Cartesian plane $(B_{\mathrm{opt}}/\Delta f;\ B_{\mathrm{Rx}}/R_S)$ for PM-QPSK modulation and $\Delta f = 33.3$ GHz. Back-to-back setup with noise loading.

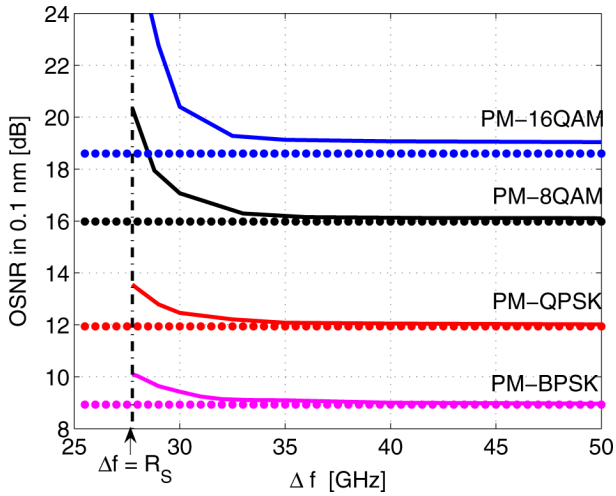

Fig. 4. Required OSNR granting $\mathrm{BER} \leq 4 \cdot 10^{-3}$ versus Δf using optimum filtering. Back-to-back setup with noise loading (solid lines). Dotted lines refer to single subcarrier performance with ideal Rx based on matched filter.

condition [26]. Moreover, tight electrical filtering helps in reducing the unwanted aliasing effects in the ADC [11].

Fig. 4 shows the back-to-back performance for all modulation formats, in terms of OSNR needed to achieve $\mathrm{BER} = 4 \cdot 10^{-3}$, as a function of Δf. The OSNR requirements at $\Delta f = 50$ GHz, where the impact of cross-talk is negligible, are 9 dB for PM-BPSK, 12 dB for PM-QPSK, 16.1 dB for PM-8QAM and 19 dB for PM-16QAM. While PM-BPSK and PM-QPSK show a limited OSNR penalty of less than 1.5 dB when decreasing Δf down to the baud rate (27.75 GHz), for PM-8QAM and PM-16QAM keeping the penalty to within 1.5 dB requires higher values of Δf (29 GHz and 30 GHz, respectively).

Fig. 5 shows the BER behavior with respect to OSNR for the four modulation formats and two values of subcarrier spacing ($\Delta f = 33.3$ and $\Delta f = 50$ GHz) together with single subcarrier performance with ideal Rx, as a reference. Focusing on the target $\mathrm{BER} = 4 \cdot 10^{-3}$, we can notice that the penalty with

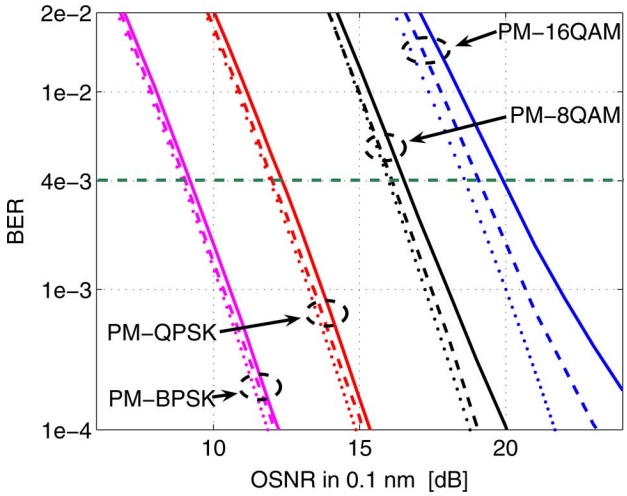

Fig. 5. BER versus OSNR in 0.1 nm for the three considered modulation formats. Back-to-back with noise loading, optimum filtering. Solid lines refer to $\Delta f = 33.3$ GHz. Dashed lines refer to $\Delta f = 50$ GHz. Dotted lines refer to single subcarrier ideal Rx based on matched filter.

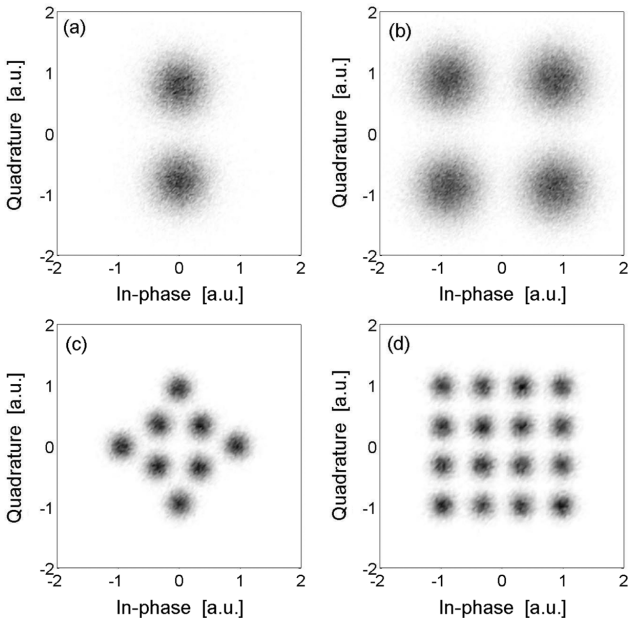

Fig. 6. Scattering diagrams for the PM-BPSK (a), PM-QPSK (b), PM-8QAM 8c) and PM-16QAM (d) in back-to-back setup with noise loading. optimum filtering. $\Delta f = 33.3$ GHz. $\mathrm{BER} = 4 \cdot 10^{-3}$.

respect to the single subcarrier case increases with the constellation cardinality, as shown in Table I.

Finally, as qualitative results, in Fig. 6 we show the scattering diagrams on a single polarization for the four analyzed modulation formats obtained in back-to-back when $\Delta f = 33.3$ GHz and $\mathrm{BER} = 4 \cdot 10^{-3}$. Fig. 7 shows the spectrum of a PM-QPSK superchannel at $\mathrm{BER} = 4 \cdot 10^{-3}$ (corresponding to $\mathrm{OSNR} = 12.1$ dB) plotted with a resolution bandwidth of 0.1 nm. Similar spectra are obtained for all modulation formats.

V. Maximum Reach versus Capacity

After identifying the OSNR sensitivity of the modulation formats under analysis, we proceeded by studying the effects of nonlinear propagation on the system setup described in

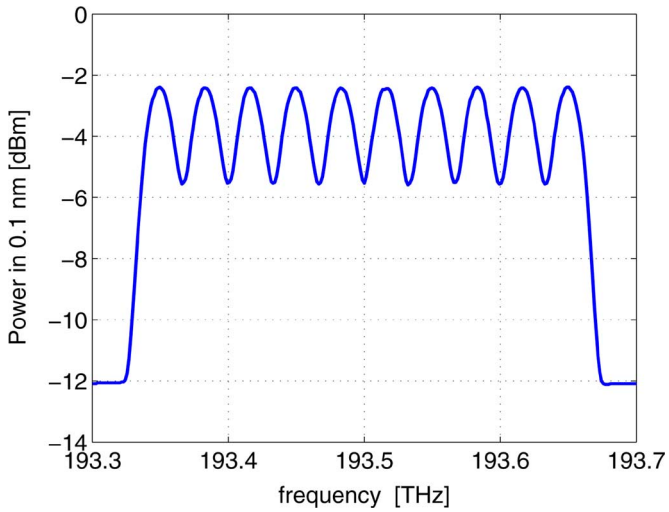

Fig. 7. Spectrum of a PM-QSPK superchannel with $\Delta f = 33.3$ GHz. $\mathrm{BER} = 4 \cdot 10^{-3}$ corresponding to $\mathrm{OSNR} = 12.1$ dB. The spectrum resolution bandwidth is 0.1 nm.

Fig. 2(a). For each modulation format, we varied the transmitted power per subcarrier (P_{Tx}) from -5 up to $+5$ dBm and propagated a comb of subcarriers over the link described in Section III. We carried out this analysis for different values of Δf, starting from 50 GHz down to the minimum tolerable subcarrier spacing, defined as the value of Δf with a penalty lower than 1.5 dB with respect to the single subcarrier case, corresponding to 27.75 GHz for PM-BPSK and PM-QPSK and 29 GHz for PM-8QAM. For PM-16QAM we also used 29 GHz, with a penalty slightly higher than 1.5 dB.

Decreasing Δf implies a reduction in bandwidth occupation, corresponding to an increase in spectral efficiency: $\mathrm{SE} = 2 \cdot M R'_S / \Delta f$, where M is the number of bit/symbol of the constellation on each polarization and $R'_S = 25$ Gbaud is the net payload baud-rate. Values of SE vary from 1 up to 1.8 bit/s/Hz for PM-BPSK ($M = 1$), 2 up to 3.6 bit/s/Hz for PM-QPSK ($M = 2$), from 3 up to 5.2 bit/s/Hz for PM-8QAM ($M = 3$) and from 4 up to 6.9 bit/s/Hz for PM-16QAM ($M = 4$). In order to express the results in terms of capacity, as well, we defined a total available bandwidth B_{av}, equal to approximately 4 THz (32 nm) in the C-band when using EDFAs. Consequently, the total link capacity is $\mathrm{C} = \mathrm{SE} \cdot \mathrm{B_{av}}$. Note that we have neglected guard-bands between superchannels, essentially because any choice would have been arbitrary. This way, the overall capacity is slightly overestimated. However, this is true for all formats and in any case the impact of this approximation is small. Note also that the maximum reachable distance was evaluated simulating the propagation of 10 subcarriers only. When extrapolating the results to the entire C-band, we implicitly assume that the nonlinear influence of subcarriers beyond $(5 \cdot \Delta f)$ away from the center channel is negligible.

For each modulation format and value of Δf we were able to assess the maximum reachable distance $L_{\max}$, for a defined span loss A_{span}, still granting $\mathrm{BER} \leq 4 \cdot 10^{-3}$. From this analysis we can estimate the robustness to nonlinearity of each analyzed modulation format over both considered fibers. Figs. 8–10 show a sub-set of these results obtained when $\Delta f = 33.3$ GHz.

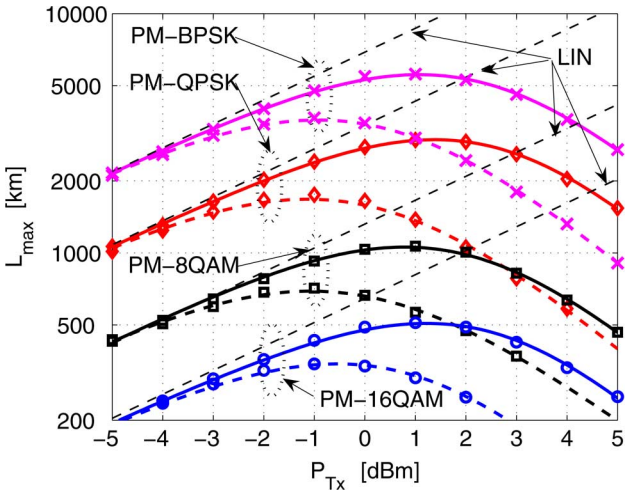

Fig. 8. Maximum reach with $\mathrm{BER} \leq 4 \cdot 10^{-3}$, $A_{\mathrm{span}} = 25$ dB and $\Delta f = 33.3$ GHz for the four considered modulation formats: PM-BPSK (crosses), PM-QPSK (diamonds), PM-8QAM (squares) and PM-16QAM (circles). Solid (SSMF) and dashed (NZDSF) lines are obtained using LMS fitting of simulation results. Linear propagation performance is shown as reference (dashed lines).

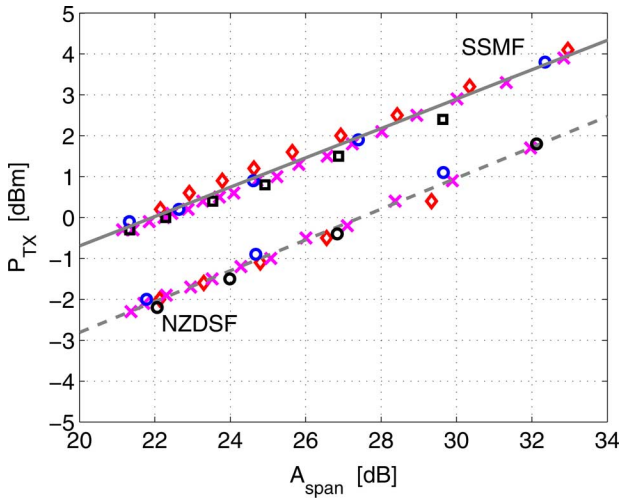

Fig. 9. Transmission power versus A_{span} needed for the maximum reach with $\mathrm{BER} \leq 4 \cdot 10^{-3}$ and $\Delta f = 33.3$ GHz for PM-BPSK (crosses), PM-QPSK (diamonds), PM-8QAM (squares) and PM-16QAM (circles). Solid (SSMF) and dashed (NZDSF) lines are obtained using LMS fitting of simulation results.

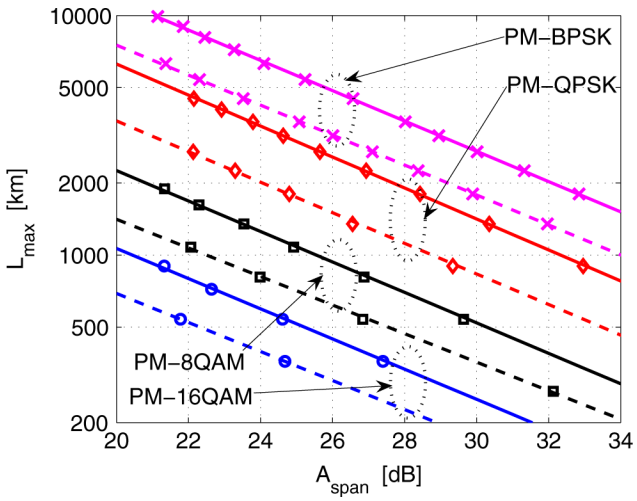

Fig. 10. Maximum reach with $\mathrm{BER} \leq 4 \cdot 10^{-3}$ and $\Delta f = 33.3$ GHz versus A_{span} for PM-BPSK (crosses), PM-QPSK (diamonds), PM-8QAM (squares) and PM-16QAM (circles). Solid (SSMF) and dashed (NZDSF) lines are obtained using LMS fitting of simulation results.

Similar curves have been obtained for all other values of subcarrier spacing, so that the comments we propose regarding these results can be considered to be quite general and essentially independent of subcarrier spacing.

In Fig. 8 we show the results of $L_{\max}$ versus P_{Tx} with $\Delta f = 33.3$ GHz, for a value of $A_{\mathrm{span}} = 25$ dB, that is typical for terrestrial links. From a qualitative analysis of this picture, we can deduce that, for both fiber types, the optimum transmission power $P_{\mathrm{Tx,opt}}$ corresponding to the maximum reach $L_{\max}$ is practically the same for all four modulation formats: about -1 dB for NZDSF and 1 dB for SSMF. For comparison, the behavior in the linear regime is plotted as well (dashed lines labeled 'LIN'). We call $L_{\mathrm{max,lin}}$ the distance reachable in the linear regime using $P_{\mathrm{Tx,opt}}$. We can then define the *nonlinear penalty* for each considered scenario as the ratio between the maximum reach in the nonlinear and linear regime: $L_{\max}/L_{\mathrm{max,lin}}$. In Table II we report the value of the nonlinear penalty for the eight analyzed scenarios. We point out that the nonlinear penalty is very similar (close to 2/3) in all cases. This circumstance suggests that there may be a fundamental explanation for this common behavior of all four formats and further investigation is currently underway.

The optimum transmitted power per subcarrier does not depend on the modulation format, but it depends on the fiber type and on the span loss, as shown in Fig. 9, where the optimum transmitted power $P_{\mathrm{Tx,opt}}$ is plotted versus A_{span} for $\Delta f = 33.3$ GHz. It can also be observed that the optimum transmitted power grows linearly with respect to span loss. The slope of such a growth can be estimated as close to 1/3 dB/dB and applies to both fiber types. The gap between the values related to SSMF and the ones related to NZDSF is therefore independent of the modulation format and of the span loss and its value can be estimated about 2 dB. Clearly, the better performance of SSMF is due to its smaller nonlinear coefficient (1.3 1/W/km with respect to 1.5 1/W/km), but also to its larger dispersion coefficient (16.7 ps/nm/km with respect to 3.8 ps/nm/km). In fact, higher dispersion appears to mitigate nonlinear impact [27], [28].

The larger the span loss, the larger is the optimum transmitted power, because the maximum reach decreases and a larger power value can be tolerated. Such a behavior is depicted in Fig. 10 where the maximum reachable distance $L_{\max}$ is plotted versus the span loss A_{span} at the optimum transmitted power $P_{\mathrm{Tx,opt}}$ for $\Delta f = 33.3$ GHz. In Fig. 10, it can be observed that the behavior of maximum reach on a logarithmic scale versus the span loss expressed in dB is linear for all the considered scenarios and the slope is the same: it can be estimated as being close to $-2/3\ 10 \cdot \log(\mathrm{km})/\mathrm{dB}$. The lines are shifted in the vertical direction depending on the modulation format because of their different respective sensitivity. Moreover, the lines are vertically shifted according to fiber type because of their different nonlinear behavior [27], [28].

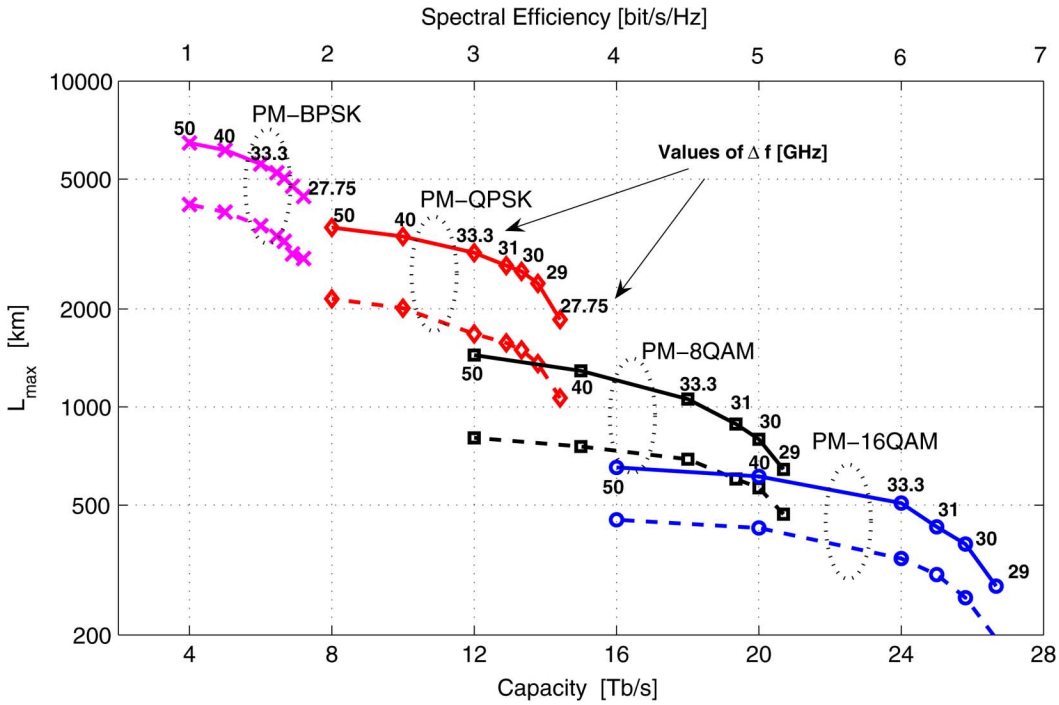

Fig. 11. Maximum reach with $\mathrm{BER} \leq 4 \cdot 10^{-3}$ versus Capacity in the C-band (bottom axis) and Spectral efficiency (top axis) for PM-BPSK (crosses), PM-QPSK (diamonds), PM-8QAM (squares) and PM-16QAM (circles). Lines are obtained connecting simulation results. Solid lines refer to SSMF and dashed lines refer to NZDSF. The corresponding values of Δf in GHz are shown at the SSMF points.

A plot summarizing the overall results presented in this paper is shown as Fig. 11, where for all the modulation formats and for both analyzed fiber types the maximum reachable distance $L_{\max}$ at $\mathrm{BER} \leq 4 \cdot 10^{-3}$ and $A_{\mathrm{span}} = 25$ dB is presented as a function of both spectral efficiency and capacity. For each format, markers correspond to (left to right) $\Delta f = [1.8, 1.44, 1.2, 1.12, 1.08, 1.04] \cdot R_S$. For PM-BPSK and PM-QPSK, the rightmost dot is $\Delta f = R_S$. The corresponding values of Δf in GHz are indicated in figure at the SSMF points.

A key result of our analysis is the emergence of a *prohibited region* in the upper right part of the $L_{\max}$ versus capacity Cartesian plan, that cannot be reached by the considered setups. In other words, in this region BER values are beyond the target value of $4 \cdot 10^{-3}$. As it could be expected, requiring a greater capacity decreases the maximum reachable distance. If the capacity requirement in the C-band is limited to 4 Tb/s, then PM-BPSK with subcarrier spacing 50 GHz can be used, and the maximum reach is 6480 km for SSMF and 4140 km for NZDSF. If the capacity requirement increases, PM-BSPK can transport up to 7.2 Tb/s, corresponding to subcarrier spacing 27.75 GHz, but in this case the maximum reach is 4410 km for SSMF and 2880 km for NZDSF.

If more capacity is needed, the complexity of the transmitted constellation must forcedly grow. PM-QPSK can be used for a capacity up to 14.4 Tb/s ($\Delta f = 27.75$ GHz), then PM-8QAM up to 20.7 Tb/s ($\Delta f = 29.00$ GHz) and PM-16QAM up to 27.6 Tb/s ($\Delta f = 29.00$ GHz).

The values of maximum reach for these systems are displayed in Table III. The maximum reach hierarchy between the two considered fiber types is maintained for the four analyzed modulation formats, showing a reduction factor that is between 1.4 and 1.75 using NZDSF with respect to SSMF (see Table III). Of course, lowering the span loss, using Raman amplification and/or PSCF fibers, significantly larger distances can be reached [7], [8]. However, the general structure and hierarchy of Fig. 11 is preserved.

TABLE I
BACK-TO-BACK PENALTY AT $\mathrm{BER} = 4 \cdot 10^{-3}$ WITH RESPECT TO THE SINGLE SUBCARRIER CASE FOR THE ANALYZED SCENARIOS

Format	Δf=50 GHz	Δf=33.3 GHz
PM-BPSK	0.05 dB	0.18 dB
PM-QPSK	0.07 dB	0.25 dB
PM-8QAM	0.13 dB	0.31 dB
PM-16QAM	0.44 dB	0.65 dB

TABLE II
NONLINEAR PENALTY (RATIO BETWEEN THE MAXIMUM REACH IN NONLINEAR AND LINEAR REGIME) FOR THE ANALYZED SCENARIOS

Format	SSMF	NZDSF
PM-BPSK	0.625	0.640
PM-QPSK	0.630	0.631
PM-8QAM	0.678	0.661
PM-16QAM	0.598	0.612

Since one of the paramaters currently used to measure the performance of long-haul WDM transmission experiments is the SE-distance product [5] (or, equivalently, the capacity-distance product [16]), we report in Fig. 12 a plot of the SE-distance product achievable with each modulation format over SSMF as a function of the subcarrier spacing. This plot can be directly derived from the curves of Fig. 11. It is interesting to note that the best performing format is PM-QPSK (with 9 000 b/s/Hz·km), followed by PM-BPSK (8 500 b/s/Hz·km),

TABLE III
MAXIMUM REACH AT THE HIGHEST CAPACITY FOR EACH MODULATION FORMAT. THE LAST COLUMN SHOWS THE RATIO BETWEEN THE MAXIMUM REACH WITH SSMF AND NZDSF

Format	SSMF	NZDSF	Ratio
PM-BPSK (55.5 Gbps)	4410 km	2880 km	1.53
PM-QPSK (111 Gbps)	1890 km	1080 km	1.75
PM-8QAM (166.5 Gbps)	630 km	450 km	1.40
PM-16QAM (222 Gbps)	270 km	180 km	1.50

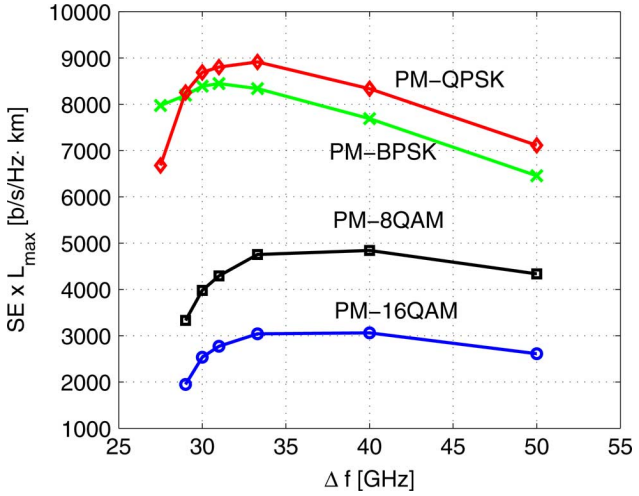

Fig. 12. Maximum SE-distance product at $\mathrm{BER} \leq 4 \cdot 10^{-3}$ versus subcarrier spacing for PM-BPSK (crosses), PM-QPSK (diamonds), PM-8QAM (squares) and PM-16QAM (circles) over SSMF. Lines are obtained connecting simulation results.

PM-8QAM (4 800 b/s/Hz·km) and PM-16QAM (3 000 b/s/Hz·km). Again, either lowering the span length and/or using Raman amplification and/or PSCF fibers, significantly larger SE-distance products can be reached [7], [8]. However, the general structure and hierarchy of Fig. 12 is preserved.

VI. CONCLUSION

We investigated the long-haul performance of Nyquist-WDM superchannels composed of PM-BPSK, PM-QPSK, PM-8QAM or PM-16QAM subcarriers, operating over SSMF or NZDSF uncompensated and amplified fiber links in the C-band. Our analysis shows the trade-off between maximum reach and capacity, and how such trade-off depends on the modulation format. In fact, only PM-BPSK can exceed 5000 km, reaching 6480 km of SSMF at a net capacity of 4 Tb/s (equivalent to 4 superchannels at 1 Tb/s) across the C band. At the other extreme, PM-16QAM can achieve a total capacity as high as 27 Tb/s (equivalent to 27 superchannels at 1 Tb/s), but the reach is then limited to 270 km only.

Other outcomes of our simulative analysis were derived from the processing of the complete set of results. They are:

- The Tx/Rx filters back-to-back optimization indicates a general law, independent of the modulation format, for the optimum bandwidth B_{opt} of the Tx optical filter and B_{Rx} of the Rx electric filter, i.e., $B_{\mathrm{opt}} = \Delta f$ and $B_{\mathrm{Rx}} = 0.5\ \mathrm{R}_S$.
- At the optimum transmitted power, the value of the maximum reachable distance $L_{\max}$ is approximately equal to 2/3 of the maximum reachable distance in linear regime, for all formats and fibers. Thus, the OSNR penalty due to fiber nonlinearity at the optimal signal launch power is ≈ 1.76 dB, that is $-10 \cdot \log_{10}(2/3)$.
- In the considered scenarios, based on the same baud-rate for all formats, we found that the optimum transmitted power per subcarrier depends on fiber type and linearly on span loss, but it is essentially independent of the modulation format.
- We verified that $L_{\max}$ linearly decreases as the span loss is increased, with a slope equal to $-2/3\ 10 \cdot \log(\mathrm{km})/\mathrm{dB}$, independently of the modulation format and of the fiber type.
- We also showed that NZDSF links experience a reduction in maximum reach of a factor of about 1.5 with respect to SSMF links, because of the higher nonlinear effects due to its larger nonlinear coefficient and also to its lower chromatic dispersion ($\mathrm{D}_{\mathrm{NZDSF}} = 3.8$ ps/nm/km compared to $\mathrm{D} =_{\mathrm{SSMF}} = 16.7$ ps/nm/km), in accordance to what argued in [27], [28].

In conclusion, the results presented in this paper appear to confirm the good performance of Terabit superchannel transmission using tightly spaced subcarriers. Since available technology was assumed, Terabit superchannels could realistically become an attractive option for the next generation of ultrahigh capacity long-haul systems.

REFERENCES

[1] K. Roberts, M. O'Sullivan, K. Wu, H. Sun, A. Awadalla, D. J. Krause, and C. Laperle, "Performance of dual-polarization QPSK for optical transport systems," *J. Lightw. Technol.*, vol. 27, pp. 3546–3559, Aug. 15, 2009.

[2] R.-J. Essiambre, G. Foschini, P. J. Winzer, and G. Kramer, "Capacity limits of fiber fiber-optic communication systems," in *Proc. OFC 2009*, San Diego, Mar. 22–26, 2009, Paper OThL1.

[3] Y. Ma, Q. Yang, Y. Tang, S. Chen, and W. Shieh, "1-Tb/s per channel coherent optical OFDM transmission with subwavelength bandwidth access," in *Proc. OFC 2009*, Mar. 22–26, 2009, paper PDPC1.

[4] R. Dischler and F. Buchali, "Transmission of 1.2 Tb/s continuous waveband PDM-OFDM-FDM signal with spectral efficiency of 3.3 bit/s/Hz over 400 km of SSMF," in *Proc. OFC 2009*, Mar. 22–26, 2009, Paper PDPC2.

[5] S. Chandrasekhar, X. Liu, B. Zhu, and D. W. Peckham, "Transmission of a 1.2-Tb/s 24-carrier no-guard-interval coherent OFDM superchannel over 7200-km of ultra-large-area fiber," in *Proc. ECOC 2009*, Vienna, Sep. 20–24, 2009, Paper PD2.6.

[6] G. Gavioli *et al.*, "Investigation of the impact of ultra-narrow carrier spacing on the transmission of a 10-carrier 1 Tb/s superchannel," in *Proc. OFC 2010*, Mar. 21–25, 2010, Paper OThD3.

[7] E. Torrengo *et al.*, "Transoceanic PM-QPSK Terabit superchannel transmission experiments at baud-rate subcarrier spacing," in *Proc. ECOC 2010*, Sep. 19–23, 2010, Paper We.7.C.2.

[8] J.-X. Cai *et al.*, "Transmission of 96 × 100 G pre-filtered PDM-RZ-QPSK channels with 300% spectral efficiency over 10 608 km and 400% spectral efficiency over 4 368 km," in *Proc. OFC 2010*, Mar. 21–25, 2010, Post-deadline paper PDPB10.

[9] B. Zhu, X. Liu, S. Chandrasekhar, D. W. Peckham, and R. Lingle, Jr., "Ultra-long-haul transmission of 1.2-Tb/s multicarrier no-guard-interval CO-OFDM superchannel using ultra-large-area fiber," *IEEE Photon. Technol. Lett.*, vol. 22, pp. 826–828, Jun. 2010.

[10] S. Chandrasekhar and X. Liu, "Experimental investigation on the performance of closely spaced multi-carrier PDM-QPSK with digital coherent detection," *Opt. Exp.*, vol. 17, no. 24, pp. 21350–21361, 2009.

[11] G. Bosco, A. Carena, V. Curri, P. Poggiolini, and F. Forghieri, "Performance limits of Nyquist-WDM and CO-OFDM in high-speed PM-QPSK systems," *IEEE Photon. Technol. Lett.*, vol. 22, pp. 1129–1131, Aug. 2010.
[12] I. Dedic, "56 Gs/s ADC: Enabling 100 GbE," in *Proc. OFC 2010*, Mar. 21–25, 2010, Paper OThT6.
[13] *Forward Error Correction for High Bit Rate DWDM Submarine Systems*, ITU-T G.975.1 Feb. 2004.
[14] A. Carena, V. Curri, P. Poggiolini, G. Bosco, and F. Forghieri, "Maximum reach versus transmission capacity for Terabit superchannels based on 27.75 Gbaud PM-QPSK, PM-8QAM or PM-16QAM," *IEEE Photon. Technol. Lett.*, vol. 22, pp. 829–831, Jun. 1, 2010.
[15] G. Charlet *et al.*, "Transmission of 81 channels at 40 Gbit/s over a transpacific-distance erbium-only link, using PDM-BPSK modulation, coherent detection, and a new large effective area fibre," in *Proc. ECOC 2008*, Sep. 21–25, 2008, Paper Th.3.E.3.
[16] G. Charlet *et al.*, "Transmission of 16.4-bit/s capacity over 2550 km using PDM QPSK modulation format and coherent receiver," *J. Lightw. Technol.*, vol. 27, pp. 153–157, Feb. 1, 2009.
[17] J. Yu, X. Zhou, and M. Huang, "8 × 114 Gbit/s, 25 GHz-spaced, PolMux-RZ-8QAM straight-line transmission over 800 km of SSMF," in *Proc. ECOC 2009*, Vienna, Sep. 20–24, 2009, Paper P4.02.
[18] A. H. Gnauck *et al.*, "10 × 112-Gb/s PDM 16-QAM transmission over 1022 km of SSMF with a spectral efficiency of 4.1 b/s/Hz and without optical filtering," in *Proc. ECOC 2009*, Vienna, Sep. 20–24, 2009, Paper 8.4.2.
[19] X. Liu *et al.*, "Multi-carrier coherent receiver based on a shared optical hybrid and a cyclic AWG array for Terabit/s optical transmission," *IEEE Photon. J.*, vol. 2, pp. 330–337, Jun. 2010.
[20] V. Curri, P. Poggiolini, A. Carena, and F. Forghieri, "Dispersion compensation and mitigation of non-linear effects in 111 Gb/s WDM coherent PM-QPSK systems," *IEEE Photon. Technol. Lett.*, vol. 20, pp. 1473–1475, Sep. 2008.
[21] G. Gavioli *et al.*, "100 Gb/s WDM NRZ-PM-QPSK long-haul transmission experiment over installed fiber probing non-linear reach with and without DCUs," in *Proc. ECOC 2009*, Vienna, Sep. 20–24, 2009, Paper 3.4.2.
[22] D. van den Borne, V. A. J. M. Sleiffer, M. S. Alfiad, S. L. Jansen, and T. Wuth, "POLMUX-QPSK modulation and coherent detection: The challenge of long-haul 100 G transmission," in *Proc. ECOC 2009*, Sep. 20–24, 2009, Paper 3.4.1.
[23] D. Hoffman, H. Heidrich, G. Wenke, R. Langenhorst, and E. Dietrich, "Integrated optics eight-port 90° hybrid on LiNbO3," *J. Lightw. Technol.*, vol. 7, pp. 794–798, May 1989.
[24] A. Carena, V. Curri, P. Poggiolini, and F. Forghieri, "Dynamic range of single-ended detection receivers for 100 GE coherent PM-QPSK," *IEEE Phot. Technol. Lett.*, vol. 20, pp. 1281–1283, Aug. 2008.
[25] Y. Han and G. Li, "Coherent optical communication using polarization multiple-input-multiple-output," *Opt. Exp.*, vol. 13, no. 19, pp. 7527–7534, 2005.
[26] S. Benedetto and E. Biglieri, *Principles of Digital Transmission: With Wireless Applications*. New York: Kluwer, 1999.
[27] A. Carena, G. Bosco, and V. Curri, "Coherent polarization-multiplexed formats: Receiver requirements and mitigation of fiber non-linear effects," in *Proc. ECOC 2010*, Torino, Sep. 19–23, 2010, Paper Mo.2.C.1.
[28] V. Curri, P. Poggiolini, G. Bosco, A. Carena, and F. Forghieri, "Performance evaluation of long-haul 111 Gb/s PM-QPSK transmission over different fiber types," *IEEE Photon. Technol. Lett.*, to be published.

Gabriella Bosco was born in Ivrea, Italy, in 1973. She received the Degree in telecommunication engineering in 1998 (thesis on the non-linear effect of the propagation in WDM optical systems) and the Ph.D. in electronic and communication engineering in 2002 (thesis on the performance analysis of optical communication systems), both from Politecnico di Torino, Italy. In 2000 she was a visiting researcher at OCPN (Optical Communication and Photonic Network) group at University of California at Santa Barbara (CA), directed by Prof. Blumenthal, working on polarization-mode dispersion monitoring techniques. She currently holds a post-doctoral position in the Optical Communication Group at the Department of Electronics of Politecnico di Torino. Her main research interests are focused on the performance analysis of optical transmission systems and the application of DSP techniques in optical links. She co-authored more than 70 papers in leading journals and conferences.

Vittorio Curri was born in Ivrea (Italy) in 1970. He received the Laurea degree *cum laude* in electrical engineer in 1995, and the Scientific Doctoral degree in optical communications in 1999, both at Politecnico di Torino, Torino, Italy. He is currently Assistant Professor at Dipartimento di Elettronica, Politecnico di Torino, Torino, Italy. He has been visiting researcher at Stanford University and UC at Santa Barbara in 1997–98. He has been a member of R&D department of Artis Software in 1998–2002. He is a member of the Board of ATS Srl.

His major research interests are fiber nonlinearities, performance estimation, advanced modulation formats, Raman amplification and simulation and modeling of optical communication systems.

Dr. Curri is an IEEE member since 1999 and has co-authored more than 60 technical publications.

Andrea Carena was born in Carmagnola, Italy, in 1970. He received the M.Sc. and Ph.D. degrees in electronic engineering from Politecnico di Torino, Italy, in 1995 and 1998 respectively. During his Ph.D. studies, he spent one year in the Optical Communication and Photonic Network group directed by Prof. Blumenthal working in the realization of OPERA, an optical label swapping network testbed. From 1998 to 2003, he was a post-doc at Dipartimento di Elettronica, Politecnico di Torino. His research has been focused on optical communication system performance evaluation, non-linear effects in fiber propagation and algorythm for computer simulation of fiber propagation. He also collaborated in the development and implementation of OptSim, an optical transmission system simulator. Since 2004, he has been assistant professor in the Optical Communication Group at Politecnico di Torino.

His current research interests are in the field of physical layer design of fiber-optic high-speed transmission systems (100 Gbps and beyond) including high order modulation formats, coherent detection, Nyquist-WDM for Terabit Superchannel implementation, and fiber nonlinearities modeling. He co-authored more than 60 scientific publications.

Pierluigi Poggiolini was born in 1963 in Torino, Italy. He received the M.S. degree "cum laude" in 1988 and the Ph.D. degree in 1993, both from Politecnico di Torino.

From 1988 to 1989 he was with the Italian State Telephone Company research center CSELT. From 1990 to 1995 he was a visiting Scholar and then a Post-Doctoral Fellow at the Optical Communications Research Laboratory of Stanford University, where he worked on the STARNET and CORD optical network research projects, funded by NSF and ARPA respectively. Since 1998 he has been an Associate Professor at Politecnico di Torino. He has published over two hundred papers in leading journals and conferences. His current research interests include long-haul coherent transmission systems, non-linear fiber effects and modeling and simulation of optical communications systems and networks.

Dr. Poggiolini was awarded he international Italgas Prize (now ENI proze) in 1998. Since 2006 he has been an elected member of the Academic Senate of Politecnico di Torino.

Fabrizio Forghieri was born in Modena, Italy. He received the Doctor of Engineering degree in electrical engineering *(summa cum laude)* from the University of Pisa, Italy, and the M.A. and Ph.D. degrees in electrical engineering from Princeton University, Princeton, NJ.

From 1993 to 1997, he has been with AT&T Bell Laboratories at first, and then with AT&T Labs Research, working on modeling of nonlinear optical effects in fibers and WDM lightwave systems and networks. From 1997 to 2001 he has been with the Lightwave Transmission Systems R&D Department of Pirelli Cavi & Sistemi. In 2001 he joined Cisco Photonics Italy, where he is currently responsible for Lightwave Systems Research.